

Neutron Stars Mass-Radius relationship and Electromagnetic follow-up of Kilonovae

D. Barba González, M. A. Pérez-García

Department of Fundamental Physics & IUFFyM, University of Salamanca, E-37008 Spain

When two Neutron Stars collide a multi-band electromagnetic emission, known as Kilonova (KN), follows being powered by the radioactive decay of ejecta products. In this contribution we discuss how the equation of state of dense matter, impacts the mass and velocity in the KN ejecta and thus its light curve. Using this information encoded in the stellar mass-radius relationship, we elaborate on how the future experimental observations in photon channels, in addition to complementary multimessenger probes, could provide a new and more detailed insight into the equation of state of nuclear matter.

1 Introduction

When two Neutron Stars (NSs) in a binary system, a BNS, coalesce and merge, they are expected to produce a multimessenger signal: gravitational waves (GW), photons from an electromagnetic (EM) counterpart and even neutrinos. One example of such event was the observation of a rapidly fading EM transient in the galaxy NGC 4993, which was spatially coincident¹ with GW170817. The optical and infrared emission, known as Kilonova (KN) or macronova, was named AT2017gfo. It was possible to identify line features in the spectra, consistent with the presence of light r-process elements (atomic masses of $A = 90\text{--}140$) powering the emission. In addition, a gamma-ray burst GRB170817A, was also detected. Since then it is now expected that many detections of this kind or similar ones i.e. Black Hole and NS (BHNS) mergers will follow in the future. An updated BNS rate¹ after the discovery of GW170817 leads to the expectation of potentially detectable dozens of events per year by LIGO/Virgo O4 and O5 runs.

In order to capture the challenging optical counterpart of a BNS merger, it is crucial to develop an alert system allowing observers to point in the right direction in the sky, obviously before it has faded away and ideally before the time it peaks. The community has gained valuable experience thanks to the historical event GW170817 localised optically in a sky area of around 30 square degrees within hours of its appearance. Typically, light curve peak values are obtained at times t_{peak} ranging between tenths of a day and a day. The alert system GraceDB², a communication node that connects LIGO and Virgo analysis pipeline, sends an alert to astronomers when a promising binary GW signal has been detected and located in the sky. Although challenging, detecting these EM counterparts is key to shed light on some relevant physical processes taking place, such as dynamical and post-merger ejection, neutron capture and thermalization in the ambient matter. Existing and future missions, like for example MAAT³ in the GTC (Spain) will be able to provide an agile response and deeper knowledge in this field. In this contribution we discuss how KNe can serve yet as another additional complementary constraint to the equation of state of neutron star matter, particularly through the light curve and spectra as measured by existing and future missions.

2 NS equation of state and key KN properties

The equation of state (EoS) of nuclear matter describes the behavior of the matter inside NSs. Typically these objects have a mass (M) up to a maximum value $M_{max} \sim 2M_{\odot}$ and a radius (R) in the 10 – 13 km range. Constraints on both quantities have been provided in a series of world-wide experimental efforts⁴. These objects appear as solutions of the stellar structure equations from General Relativity (GR) and their computed $M(R)$ values display some spread due to the poorly known high density matter EoS. In particular, it is not yet known what are the actual degrees of freedom suitable for its description, i.e. whether matter inside remains under the form of nucleons or perhaps deconfined as quarks. NSs are born in the aftermath of a Supernova explosion displaying a large velocity kick and distribute mostly towards the center of the galaxies. Further into the NS description, its layered structure can be mainly explained from two regions: an external crust and a central core. It is believed that up to nearly 99% of the NS mass resides in the latter under the form of nucleons, hyperons and alike species although if high densities are in excess of $\sim 6 \times 10^{14}$ g/cm³ a quark deconfined state may appear⁵. From the population studies of Galactic double NSs (DNSs) it appears that $\simeq 98\%$ of all merging DNSs will have a mass ratio, q , close to unity⁶ $q < 1.1$. Recent studies⁷ find that the weighted mean masses of the primary and companion stars are respectively $(1.439 \pm 0.036)M_{\odot}$ and $(1.239 \pm 0.020)M_{\odot}$. In addition, the surface magnetic field strength in the primary stars of the DNSs is $B \sim 10^{10}$ G, and the spin period is $P \sim 50$ ms. Due to the fact that the NS in the BNS events under scrutiny will share these general characteristics it is important to see what information the EM counterparts can yield. The gravitational and baryonic masses are two quantities that determine the binding energy (BE) of the NS. Namely, the gravitational mass is $m_G(R) = M = \int_0^R 4\pi r^2 \epsilon(r) dr$ where $\epsilon(r)$ is the energy density at a radial distance r from the center and the baryonic mass $M_B = M^* = m_0 \int_0^R 4\pi r^2 [1 - 2Gm_G(r)/rc^2]^{-1/2} n(r) dr$ where m_0 is the mass of a baryon and $n(r)$ is the baryon (nucleon) number density. The binding energy of the NS is $BE = (M^* - M)c^2$ and typically $BE = |BE|$ is taken as a positive quantity.

In the literature, some universal relations between the BE and C have been proposed, such as that⁸ based on the radius of a $1.4M_{\odot}$ NS, $R_{1.4}$, $M^* = M + R_{1.4}^{-1} \times M^2$, with 1.8% relative error. Note that the $1.4M_{\odot}$ selection is close to the most probable for primary companions in DNSs. In order to illustrate our findings we consider two EoS i.e. DD2 and SFHo⁹, whose $M(R)$ relationship is shown in Fig.(1) left panel. For SFHo it is found a saturation density $n_0 = 0.1583$ fm⁻³, nuclear incompressibility $K = 245.4$ MeV, symmetry energy $J = 31.57$ MeV and a logarithmic derivative of the symmetry energy $L = 47.10$ MeV. For the DD2 $n_0 = 0.1491$ fm⁻³, $K = 242.7$ MeV, $J = 31.78$ MeV and $L = 55.19$ MeV. Using existing data¹⁰ from BNS simulations we obtain $R_{1.4}^{DD2} = 13.5 \pm 0.1$ km, $R_{1.4}^{SFHo} = 11.8 \pm 0.1$ km, see Fig.(1) right panel. Considering the sum of BE of both NSs described by a given EoS, $BE_1 + BE_2$, we arrive at values for DD2: $BE_1 + BE_2 = 0.25 \pm 0.04M_{\odot}$ and SFHo: $BE_1 + BE_2 = 0.28 \pm 0.04M_{\odot}$ which fulfill the fitted form¹¹ $\frac{BE_i}{M_i} = -0.0130 + 0.618C_i + 0.267C_i^2$ where $C_i = \frac{GM_i}{R_i c^2}$ is the compactness. They retain the $M(R)$ relationship from C and M values.

As shown in GR simulations¹² the ejected mass in a violent BNS merger is mostly stripped from the inner and outer crust of the NSs and will be determined by the energetics of the collision and the actual amount of matter in the crust. In a NS the neutron rich crust displays a large set of inhomogeneous substructures ranging from lattice nuclei to *pasta phases*¹³. In the thin-crust approximation $M_{crust} \approx \frac{4\pi R^3 P_t}{c^2 C} [1 - 2C]$ where P_t is the EoS dependent pressure transition from the crust-core regions¹⁴. There is a large sensitivity to the EoS in the crust mass value, being smaller for heavier stars. Recent Bayesian analysis¹⁵ provide values for the transition density $n_t = 0.072 \pm 0.011$ fm⁻³ and the transition pressure $P_t = 0.339 \pm 0.115$ MeV fm⁻³. The resulting crust masses $M_{crust}^{DD2} = 0.038M_{\odot}$ and $M_{crust}^{SFHo} = 0.024M_{\odot}$. In addition, the number of baryons must be conserved $N_1^* + N_2^* = N_{remnant}^* + N_{eject}^*$.

The complex dynamics of the BNS merger and its ejecta are studied using GR numerical

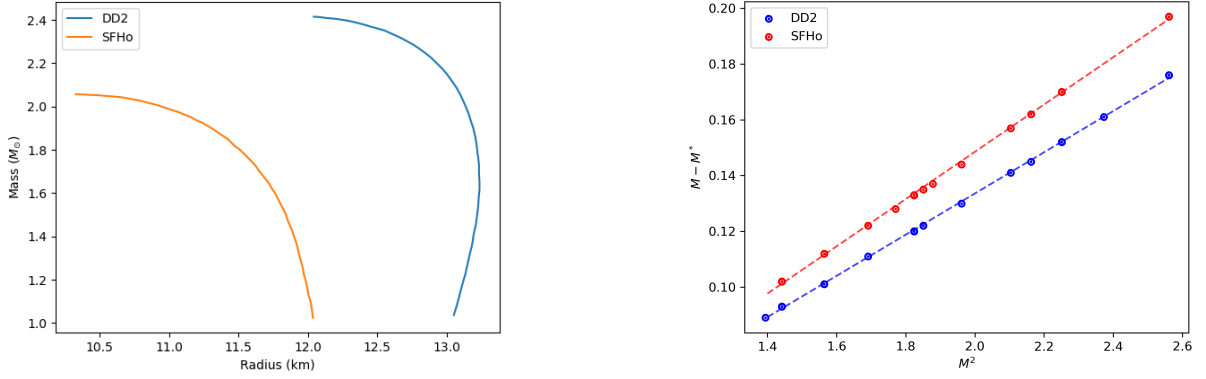


Figure 1 – $M(R)$ relationship for the DD2 and SFHo EoS (left) and BE as a function of M^2 (right)

simulations with a number of approximations regarding neutrino transport and microphysics. The output is obtained by determining the relevant parameters modelling the KN emission, including the mass, M_{ej} , and velocity, v_{ej} , of the ejecta, which are fitted¹⁰ (with some uncertainty, see parameterizations) to functional forms depending on both objects in the BNS (1, 2),

$$\frac{M_{\text{ej}}^{\text{fit}}}{10^{-3}M_{\odot}} = \left[a \left(\frac{M_2}{M_1} \right)^{1/3} \left(\frac{1-2C_1}{C_1} \right) + b \left(\frac{M_2}{M_1} \right)^n + c \left(1 - \frac{M_1}{M_1^*} \right) \right] M_1^{*+(1 \leftrightarrow 2)+d}, \quad (1)$$

$$v_{\text{ej}} = \sqrt{v_{\rho}^2 + v_z^2}, \quad v_{\rho,z} = \left[a_{\rho,z} \left(\frac{M_1}{M_2} \right) (1 + c_{\rho,z} C_1) \right] + (1 \leftrightarrow 2) + b_{\rho,z}. \quad (2)$$

We plot in Fig.(2) left panel, the ejected mass as a function of gravitational masses M_1, M_2 for $M_i \in [1.2, 1.6]$ in our analysis with the DD2 EoS. As a rule of thumb we see that smaller mass ratio $q \equiv M_{<}/M_{>}$ provide larger M_{ej} . The experimental measurement of the KN peak bolometric luminosity and spectral time series usually depend on the conditions of transparency after the ejection of matter parameterized through the opacity, κ . For early emission, typically $\kappa \sim 0.1 \text{ cm}^2 \text{ g}^{-1}$ while for later r-powered emission κ could be a factor of 10 or more larger. The peak values and are given¹⁶ by $t_{\text{peak}} = 4.9 \text{ d} \times \left(\frac{M_{\text{ej}}}{10^{-2}M_{\odot}} \right)^{\frac{1}{2}} \left(\frac{\kappa}{10 \text{ cm}^2 \text{ g}^{-1}} \right)^{\frac{1}{2}} \left(\frac{v_{\text{ej}}}{0.1} \right)^{-\frac{1}{2}}$. For a BNS the measurable magnitudes can be fitted to the Black Body power spectrum¹ and from GW170817 some constraints appear for masses i.e. total mass $M \approx 2.74M_{\odot}$, and individual masses of $M_1 \approx (1.36 - 1.6)M_{\odot}$ and $M_2 \approx (1.17 - 1.36)M_{\odot}$. Also from this analysis marginalized over the selection methods, it was obtained that the radius of the progenitors $R_1 \sim (10.8 - 11.9) \pm 2 \text{ km}$ and $R_2 \sim (10.7 - 11.9) \pm 2 \text{ km}$ and the tidal deformability parameters $\Lambda_1 < \Lambda_2, \Lambda_1 < 500$ and $\Lambda_1 < 1000$. Under this additional input they find $\tilde{\Lambda}(310 - 345)_{-245}^{+691}$ and $R_{1.4} = 8.7 - 14.1 \text{ km}$, where the binary tidal deformability $\tilde{\Lambda}$ is defined as $\tilde{\Lambda} \equiv \frac{16}{13} \left[\frac{\Lambda_1 M_1^4 (M_1 + 12M_2)}{(M_1 + M_2)^5} + 1 \leftrightarrow 2 \right]$ which is most precisely derived.

Direct measurements from current and future missions will be able to provide time spectral series. In Fig.(2), right panel, we plot the simulated fluxes of two runs using POSSIS¹⁷ as a function of the EM rest wavelength. Run 1 (Run 2) corresponds to a $q = 1$ BNS merger of $1.4M_{\odot}$ at 40 Mpc using the output of recent simulations¹⁸ $M140140 - LK$ of DD2 (SFHo) EoS using polar/equatorial orientations. We notice that the early, agile KN follow up would be key to further constrain the EoS. The soft SFHo EoS peaks at IR, and is fainter than DD2 across the whole spectrum. Since the q values remain the same we rely to the EoS features (including secondary peak features) for wavelengths less than $\sim 1\mu\text{m}$.

To summarize, we have discussed the dependencies of the EM observables obtained from KN light curves (peak values) with $q = 1$ in order to help indirectly constrain quantities such as the $M(R), C, BE, R_{1.4}$ and thus the EoS of NS matter. In particular, the combination of

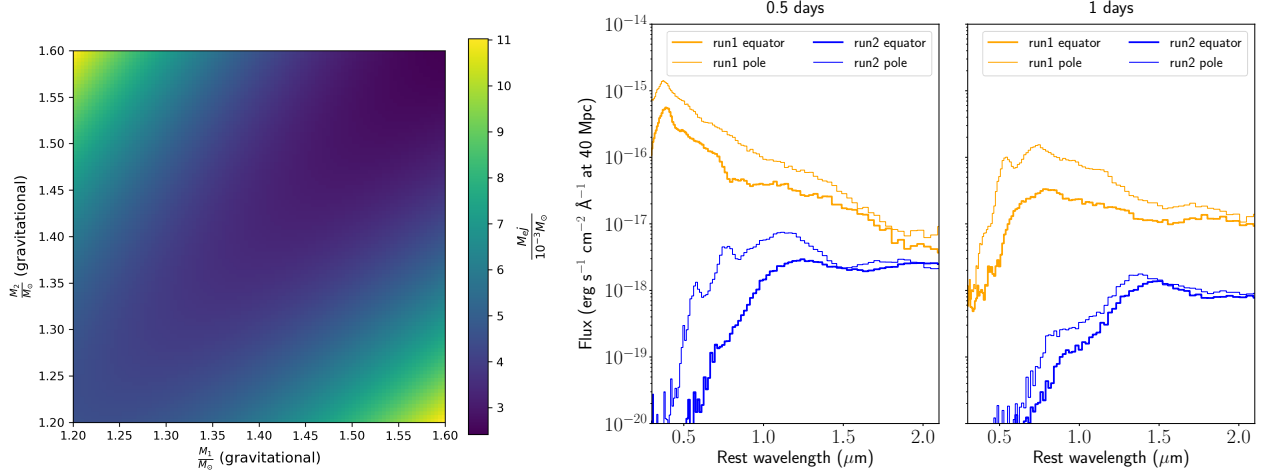


Figure 2 – (left) Ejected mass from simulation data¹⁰. (right) Simulated flux for a BNS merger using DD2 (run 1) and SFHo (run 2) EoS at 40 Mpc for polar and equatorial view angles at 0.5 d (left) and 1 d (right) after the merge.

optical/IR observations from proposed missions such as MAAT in addition to GW signals from the LIGO/Virgo collaboration, will provide complementary valuable input. Further work is in progress.

Acknowledgments

We acknowledge useful comments from C. Albertus, M. Bulla, L. Izzo and F. Prada. Spectra in Fig. (2) are courtesy of M. Bulla. This research has been supported by University of Salamanca, Junta de Castilla y León SA096P20, Spanish Ministry of Science PID2019-107778GB-I00 projects, MULTIDARK Spanish network and PHAROS COST Action CA16214.

References

1. B.P. Abbott et al., *Phys. Rev. Lett.* **119**, 161101 (2017).
2. Grace alert system, <https://gracedb.ligo.org/>.
3. F. Prada et al., <https://arxiv.org/abs/2007.01603>
4. T. Dietrich et al, *Science* **370** 1450 (2020); M. Fasano, T. Abdelsalhin, A. Maselli, V. Ferrari, *Phys. Rev. Lett.* **123**, 141101 (2019)
5. O. Ivanytskyi, M.A. Pérez García, V. Sagun et al., *Phys. Rev. D.* **100**, 103020 (2019).
6. C.M. Zhang, J. Wang, Y. H. Zhao et al, *Astronomy and Astrophysics.* **527**, A83 (2011).
7. Y. Yi-yan et al., *Chinese Astronomy and Astrophysics*, **41**, 4 (2017).
8. H. Gao, H., S. K. Ai, Z.J. Cao et al., *Front. Phys.* **15**, 24603 (2020).
9. S. Typel et al., *Phys. Rev. C* **81**, 015803 (2010); A. W. Steiner et al. *ApJ* **774** 17 (2013).
10. T. Dietrich and M. Ujevic, *Class. Quantum Grav.* **34** 105014 (2017).
11. D. S. Shao, S. P. Tang, X. Sheng et al, *Phys. Rev. D* **101**, 063029 (2020).
12. A. Bauswein, S. Goriely, H. T. Janka, *ApJ* **773** 78 (2013).
13. C. J. Horowitz, M.A. Pérez García, D. K. Berry et al., *Phys. Rev. C* **72** 35801 (2005).
14. N. Chamel and P. Haensel, *Living Rev. Relativ.* **11** 10 (2008)
15. T. Carreau. F. Gulminelli and J. Margueron, *Eur. Phys. Jour. A* **55** 188 (2019).
16. K. Kawaguchi, M. Shibata and M. Tanaka, *ApJ* **889** 171 (2020).
17. M. Bulla, *MNRAS* **489** (2019) 5037.
18. D. Radice et al., *ApJ* **869** 130 (2018).